ALEPH 92-48
PHYSIC 93-39
J. Raab and B. Wolf
9.3.1993

Measurement of the τ neutrino helicity in the decays $\tau \rightarrow \pi\nu$ and $\tau \rightarrow \rho\nu$

J. Raab and B. Wolf

Johannes Gutenberg–Universität Mainz

1 Introduction

We present a measurement of the τ neutrino helicity in the decays $\tau \rightarrow \pi\nu$, $\rho\nu$ based on data collected in 1990 and 1991 [1]. From correlated decay spectra and the constraint on the τ polarisation from the combined LEP lineshape measurements for 1990 and 1991 [2], we find that the τ neutrino helicities are the same within errors for both decays. Combining the two measurements leads to $h(\nu_\tau) \equiv \xi_{had} = -1.00 \pm 0.07 \pm 0.04$.

2 Motivation

In the Standard Model the weak charged current couples in the limit of zero mass only to left–handed particles. This $V-A$ structure is a special case of the most general allowed by Lorentz -, T - and CPT invariance [3][4]. Additional couplings affect decay rates, the polarisations and the energy spectra of the final state particles. The shape of the semileptonic τ decay spectra depend on the Michel parameter ξ which depends on all possible coupling constants. ξ turns out to be identically equal to the ν_τ–helicity for hadronic currents with unique J^{PC} quantum numbers. For mixtures of V and A is ξ always the same for all decay modes. The Standard Model $V-A$ prediction is $\xi = -1$.

The first measurement of the ν_τ–helicity was performed by ARGUS. They were able to extract $h(\nu_\tau) = -1.25 \pm 0.23^{+0.08}_{-0.15}$ from $\tau \to a_1 \nu$ decays [5].

At LEP, and particularly with the ALEPH detector, we can improve on the ARGUS measurement by using the correlated energy spectra of the π and ρ decay channels. On the Z^0 resonance the τ's are produced with mean polarisation p and opposite helicities. The decay spectra are thus functions of the production parameter p as well as ξ.

The distributions in the polarisation sensitive variable z of a τ decay product can in general be written as [6][7][8][9]:

$$\frac{1}{\Gamma}\frac{d\Gamma}{dz} \propto F(z) - p \cdot \xi \cdot G(z).$$

For the decay $\tau \to \pi\nu$, $z \equiv (2E/E_\tau - 1)$ is the cosine of the decay angle of the π relative to the τ spin in the τ CM system[1]. The functions F and G are particularly simple, $F(z) = 1$ and $G(z) = z$. In the ρ-channel we use $z \equiv \mid E_\pi - E_{\pi^0} \mid /(\mid \beta_\rho \mid E_\tau)$. F and G are rather complicated and are shown in Figure 1.

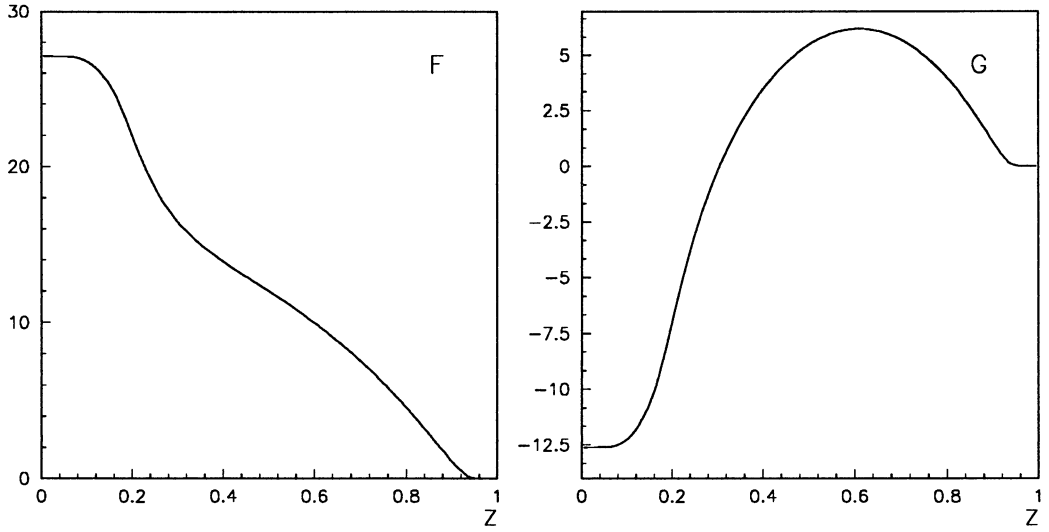

Figure 1: *The functions $F(z)$ and $G(z)$ for $\tau \to \rho\nu$ (the Breit-Wigner resonance shape of the ρ has been integrated over).*

[1] We assume $E_\tau = E_{beam}$ unless explicitely specified.

The correlated spectra can be derived from the single spectra, knowing that on average a fraction $\frac{1}{2}(1+p)$ of the τ pairs are produced with positive and the rest with negative polarisation:

$$\begin{aligned} T(z_1,z_2) = \frac{1}{\Gamma}\frac{d^2\Gamma}{dz_1 dz_2} \quad &\propto \quad \frac{1+p}{2}\left[F(z_1)-\xi_1 G(z_1)\right]\left[(F(z_2)-\xi_2 G(z_2)\right] + \\ & \quad \frac{1-p}{2}\left[F(z_1)+\xi_1 G(z_1)\right]\left[(F(z_2)+\xi_2 G(z_2)\right] \\ &= \quad F(z_1)\cdot F(z_2) + \xi_1\cdot\xi_2\cdot G(z_1)\cdot G(z_2) - \\ & \quad p\cdot\left[\xi_1\cdot G(z_1)\cdot F(z_2) + \xi_2\cdot G(z_2)\cdot F(z_1)\right] \end{aligned}$$

For ARGUS and CLEO $p = 0$ so that only the product $\xi_1 \cdot \xi_2$ could be measured there. As a consequence of the polarisation at LEP we can determine both independently.

Figure 2 illustrates that the sensitivity to ξ is greatest at the boundaries of the spectra, i.e., near the edge of phase space [7].

3 Event Selection

The analysis incorporates 18.8 pb^{-1} of data recorded by ALEPH in 1990 and 1991. We use the TCL package developed by the Wisconsin group to select and classify τ decays [10]. The preselection is identical to CLASS 15. Every track is classified by a Neural Net particle identification program as an e, μ or π candidate. Only events with two tracks, one per hemisphere, are retained. In case a π-candidate is found the corresponding hemisphere is searched for a π^0 to be combined into a ρ candidate.

Bhabha, dimuon and two-photon backgrounds are rejected essentially on the basis of total energy and acollinearity.

The TCL package provides the track energies of the μ and π candidates. The stored energy of the e candidates also includes the energy of single nearby photons. We remove this correction since we treat final state radiation semi–analytically and correct for bremsstrahlung in the detector with a resolution matrix.

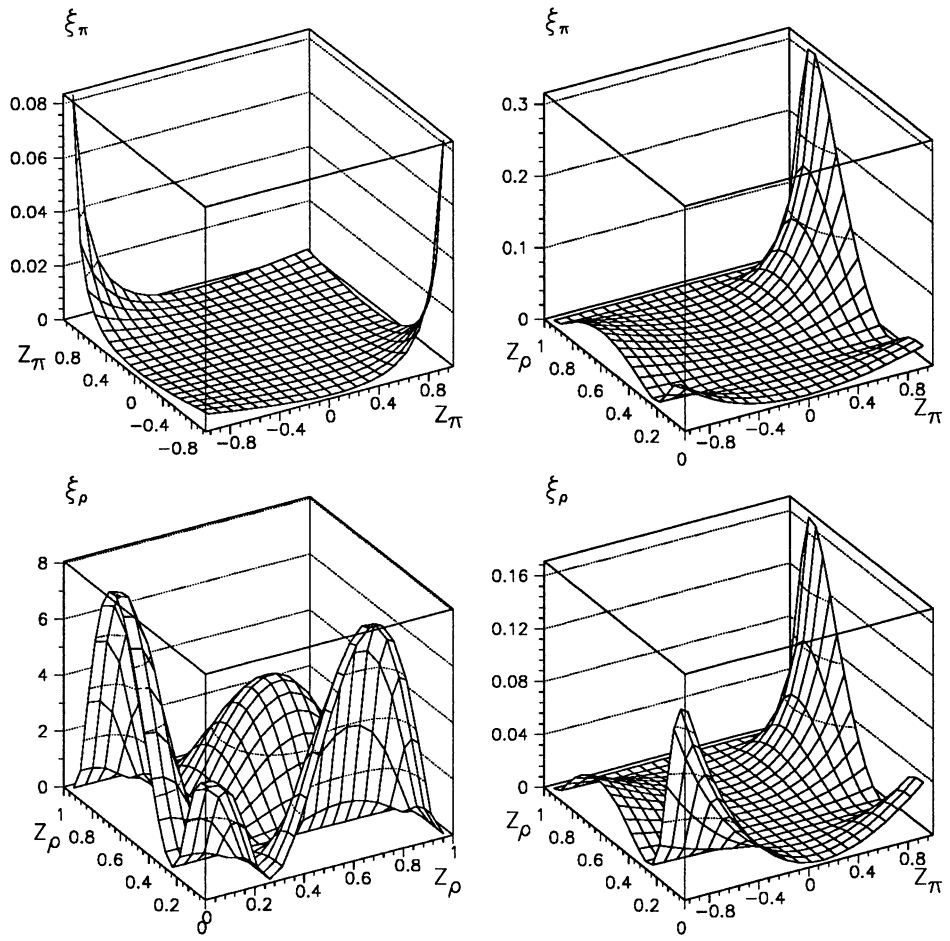

Figure 2: *The theoretical sensitivity* $S \equiv \left(\frac{\xi}{\sigma_\xi}\right)^2$. *From top left clockwise:* $S(\xi_\pi)$ *for* $\pi\pi$ *and* $\pi\rho$; $S(\xi_\rho)$ *for* $\pi\rho$ *and* $\rho\rho$.

We require in TCL jargon:

- IPRE > 0
- IBPOS = IBNEG =0.

Table 1 lists the total number of e, μ, π, and ρ candidates. They are identical to those published by [11].

The candidate events are split into two groups: those in which both hemispheres are positively identified as either e, μ, π or ρ, and those in which only one hemisphere was identified. For the ν_τ–helicity measurement we do not con-

Mode	# events 1990+91	ε	τ B[%]	non-τ B[%]	NN # events 1990+91	ε	τ B[%]	non-τ B[%]
eX	3780	0.47	1.9	1.2	3780	0.48	1.9	1.1
μX	5492	0.69	1.3	1.0	5492	0.70	1.3	1.1
πX	3438	0.60	7.1	1.4	3438	0.61	7.0	1.5
ρX	5232	0.46	5.9	0.5	5232	0.47	6.2	0.6

Table 1: *Number of candidates, acceptance (ε), and predicted backgrounds (B) for this analysis and the Neural Net (NN).*

Mode	# events 1990	ε	τ B[%]	non-τ B[%]	# events 1991	ε	τ B[%]	non-τ B[%]
$\pi\pi$	60	0.44	11.4	0.6	108	0.47	12.6	-
$\pi\rho$	170	0.36	14.5	0.2	329	0.38	12.0	0.1
$\rho\rho$	139	0.30	12.3	0.5	299	0.28	8.7	-
πX	909	0.47	7.4	1.6	1694	0.46	7.1	1.9
ρX	1302	0.37	6.2	0.6	2555	0.36	6.0	0.6

Table 2: *Event numbers, efficiency (ε), and backgrounds (B) for the hadron selection.*

sider the purely leptonic modes any further[2]. The events with a lepton on one side and a π or ρ on the other are included in the πX or ρX channels. Table 2 summarizes this *hadronic* data set.

The data are binned in steps of $\Delta z = 0.1$ for ρ and $\Delta z = 0.2$ for π.

4 Acceptance and Background

The acceptance ε is determined from MC, by folding the true energy spectra with a resolution matrix $\mathcal{R}$ and comparing them to the number of reconstructed events in each bin. The resolution matrix describes the transition from the true energy spectrum to the measured one, thus accounting for detector resolution

[2]The leptonic channels will be the subject of a future note.

and bremsstrahlung in the detector material[3]. Due to correlated cuts in classification and background rejection it is only approximately true that in each bin $\varepsilon(i,j) = \varepsilon(i) \cdot \varepsilon(j)$. In Figures 3 and 4 we show the efficiency distributions for all the modes. The bins with $\varepsilon = 1$ reflect a lack of MC statistics at the phase space bounderies. The fit takes this partly into account (see below).

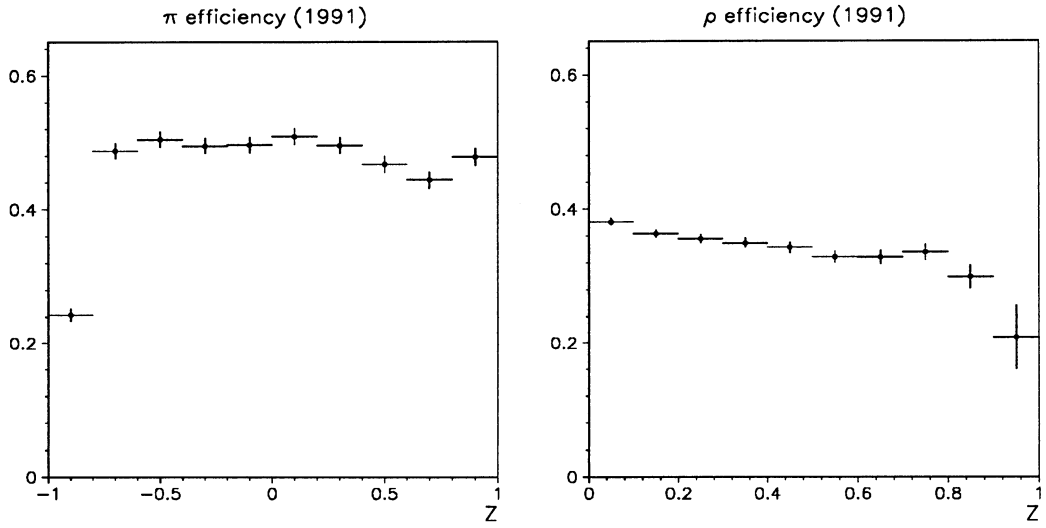

Figure 3: *Efficiencies for the single π and ρ spectra.*

The backgrounds are extracted from full MC simulations for each year of data taking. The non-τ background in each channel is determined from bhabha- , dimuon-, multihadron-, and two–photon to lepton- and to hadron events. Each sample represents at least a factor of three more in integrated luminosity than the data. The background from misidentified τ decays is taken from τ-pair simulations with six or eight times the statistics of the data.

5 The fit

The observed one- and two-dimensional distributions $N(i,m,n)$ and $N(i,j,m,n)$ in the polarisation sensitive variable z are fit to the expected spec-

[3]The energy loss due to final state radiation is not included here.

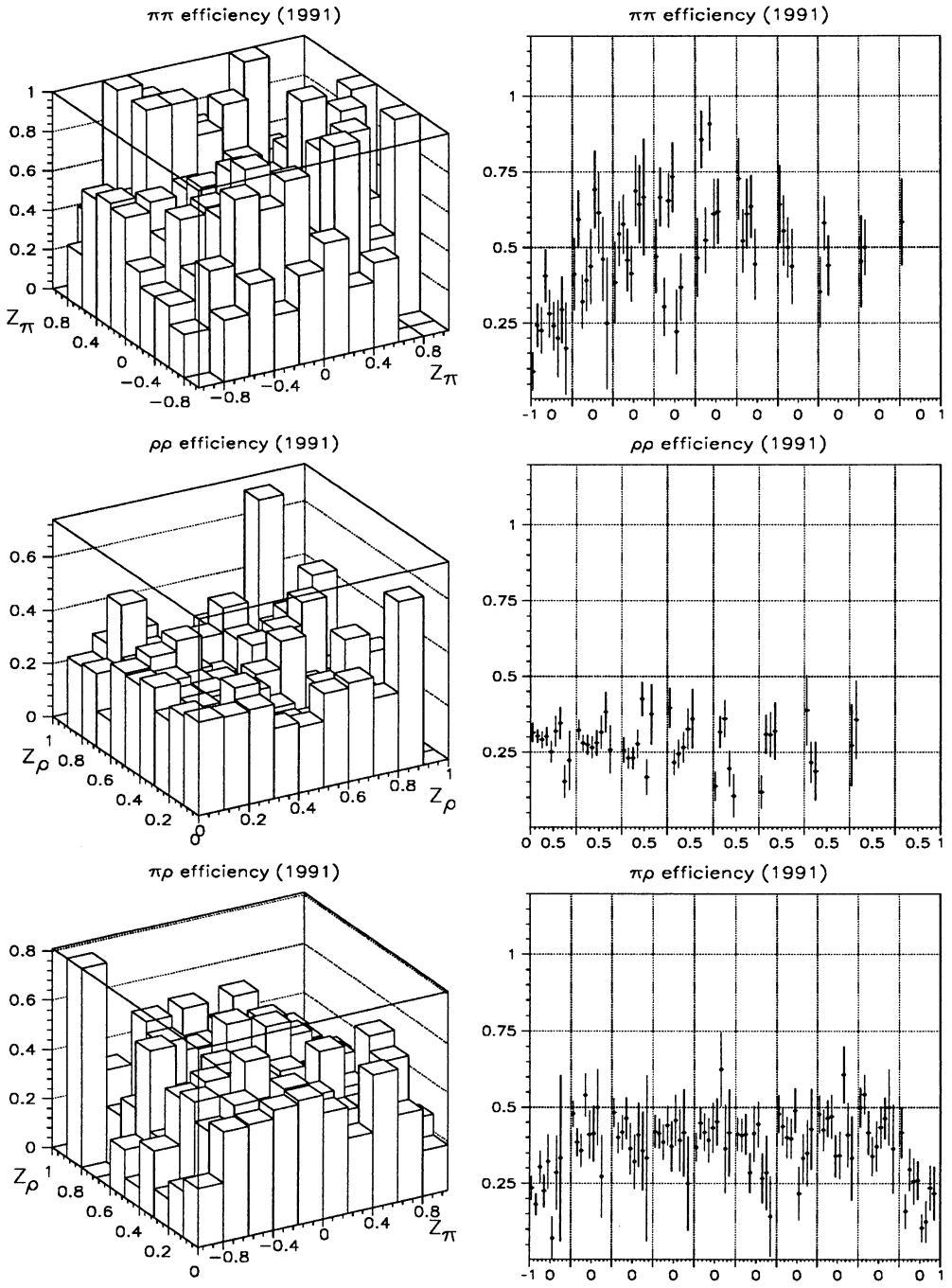

Figure 4: *Efficiencies for $\pi\pi$, $\rho\rho$ and $\pi\rho$. left: the two-dimensional distributions; right: the two-dimensional distributions as linear plots with errors. The first interval corresponds to $z_\pi = [-1., -0.8]$, the second to $z_\pi = [-0.8., -0.6]$, etc. The $\pi\pi$ and $\rho\rho$ modes are folded across the diagonal.*

trum E by minimising the negative log-likelihood of

$$\mathcal{L} = \prod_{i,j,m,n} \frac{e^{-E(i,j,m,n)} E(i,j,m,n)^{N(i,j,m,n)}}{N(i,j,m,n)!}$$

$$\ln \mathcal{L} = \sum_{i,j,m,n} [-E(i,j,m,n) + N(i,j,m,n) \ln E(i,j,m,n)].$$

The indices i, j run over all the bins in the fit range, m denotes the mode and n the dataset (here two: 1990, 1991). This choice of $\mathcal{L}$ assumes that the binned data follow Poisson statistics and $-2 \ln \mathcal{L}$ behaves asymptotically like a χ^2 with $i_{max} \times j_{max} - (k+1)$ degrees of freedom for fixed n, m and k fit parameters. The information on the polarisation from LEP (see section on results) is implemented by the addition of the Gaussian term

$$-\frac{1}{2}\left(\frac{p_{fit} - p_{LEP}}{\sigma_{LEP}}\right)^2$$

The expected spectrum E is the sum of the theoretical spectrum T corrected for final state radiation (FSR) [12], folded with efficiency and resolution matrices, ε and $\mathcal{R}$, and the predicted background B,

$$E(i,j,m,n) = \prod_{i',j'} T(i',j',m,n)\varepsilon(i',j',m,n)\mathcal{R}(i,i')\mathcal{R}(j,j') + B(i,j,m,n).$$

The correct normalisation for each mode is achieved through the requirement that the integral over the fit range yield the observed number of events therein,

$$\sum_{i,j} E(i,j,m,n) = N(m,n).$$

We assume that the background from other τ modes do not significantly influence the fit parameters. This assumption is born out by the result that we do not find a significant deviation from $V-A$.

Our approach differs from the traditional ALEPH procedure in two aspects: we fit the spectra to analytic formulae rather than to differents weights of Monte-Carlo spectra with pure polarisation states, and we use semi–analytical formulae for final state radiative corrections. The analytical fit is necessary because the standard MC τ–pair generator KORALZ does not include a general set of Michel parameters. Our treatment of FSR allows an uncompromised use

of measured track energies (this will be more relevant for the leptonic modes). We verify our method by applying the fit to the true MC spectra. Effects of FSR must be included since the τ energy before radiation is not stored on the standard MC output. A comparison between our single parameter fit results and the MC $V-A$ input parameters are given in Table 3.

mode	fit to MC	p_{in}	p_{found}	ξ_{found}
πX, $\pi\pi$, $\pi\rho$	truth	-0.116	-0.105 ± 0.016	-1.05 ± 0.03
	reconstructed		-0.098 ± 0.020	-1.01 ± 0.07
ρX, $\rho\rho$, $\pi\rho$	truth	-0.131	-0.144 ± 0.009	-1.01 ± 0.03
	reconstructed		-0.150 ± 0.017	-1.01 ± 0.06

Table 3: *Fit results to the MC truth and reconstructed spectra. The latter includes efficiency and resolution corrections, and the background subtraction.*

We make a further cross check by fitting to the polarisation in the data. All other parameters are fixed at their $V-A$ values. Table 4 shows that our results are in good agreement with those of the standard ALEPH analysis [11].

These checks illustrate that our approach is not only reliable but also consistent with the traditional method.

6 Results

Our interest is mainly in the measurement of ξ and not the production parameter p. Nevertheless, fixing the decay parameters to their Standard Model values

mode	# events	p	mode	NN # events	p
πX, $\pi\pi$, $\pi\rho$	3438	-0.135 $\pm$ 0.035	πX	3438	-0.133 $\pm$ 0.033
ρX, $\rho\rho$, $\pi\rho$	5232	-0.138 $\pm$ 0.034	ρX	5232	-0.150 $\pm$ 0.031
combined		-0.137 $\pm$ 0.025			-0.144 $\pm$ 0.023

Table 4: *Polarisation fit results in comparison with the values given by the NN analysis.*

and fitting to p provides a convenient consistency check (see Table 4).

For the simultaneous determination of ξ_π and ξ_ρ we use the full *hadronic* subsample. Thus we have a self-consistent data set and we avoid potential problems in the leptonic channels at negligible cost in sensitivity and statistical precision. The measured values for p, ξ_π, ξ_ρ and the corresponding correlation coefficients are listed in the first row of Table 5. In the second row we have used the additional information on p as extracted from the combined LEP lineshape measurements [2], $p = -2\frac{g_v/g_a}{1+(g_v/g_a)^2} = -0.143 \pm 0.013$. The next two rows contain the fit results with the assumption of "hadron"–universality, i.e., $\xi_{had} = \xi_\pi = \xi_\rho$. Figures 5 and 6 show the spectra for the data, the fit and the background.

Comment	p	ξ_π	ξ_ρ	$C(p,\xi_\pi)$	$C(p,\xi_\rho)$	$C(\xi_\pi,\xi_\rho)$	χ^2/NDOF
	-0.127	-1.02	-1.03	-0.23	-0.22	-0.21	655 / 637
	± 0.027	± 0.12	± 0.11				
with LEP	-0.140	-1.00	-1.01	-0.13	-0.12	-0.24	655 / 637
constraint	±0.012	± 0.12	± 0.11				
		ξ_{had}		$C(p,\xi_{had})$			
	-0.127	-1.02		-0.35			655 / 638
	± 0.027	± 0.07					
with LEP	-0.140	-1.00		-0.20			655 / 638
constraint	±0.012	± 0.07					

Table 5: *Results for the measurement of the ν_τ–helicity with and without the additional information from the LEP lineshape measurements. The columns labelled $C(\alpha,\beta)$ give the correlation coefficient.*

7 Systematic errors

From the formula for $\mathcal{L}$ we see that possible sources of systematic errors are inaccurate resolution, efficiency and background matrices, the binning, and the fit range.

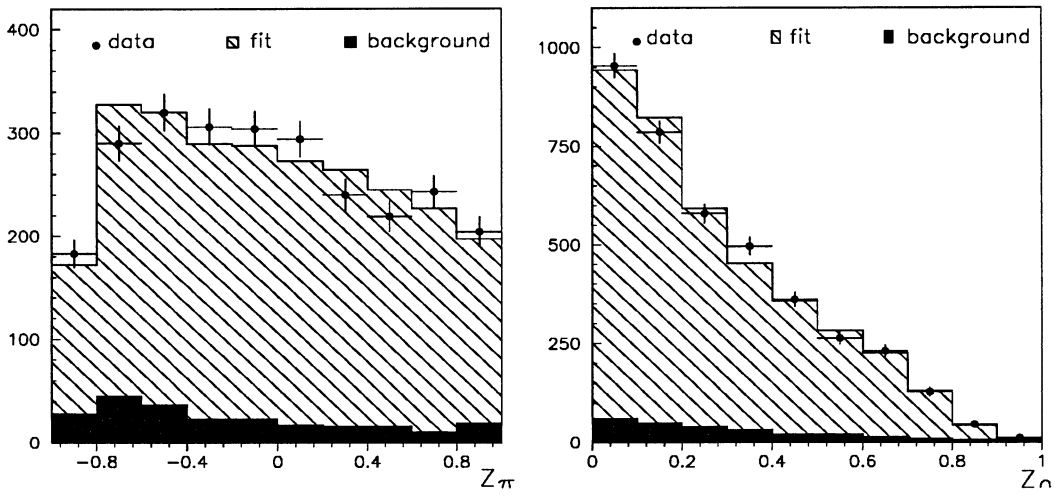

Figure 5: *Data, background and fit for single π and ρ spectra.*

The influence of the binning is two-fold. First, large bin sizes wash out the sensitive regions and too fine a binning results in many bins having no data entries. The likelihood $\mathcal{L}$ correctly accounts for the latter case. Second and more relevant is the effect of the binning on the efficiency matrices. With a fine grained grid it frequently happens that the number of MC entries are too few to determine the effficiency to less than 10%. We determine the errors due to the binning a) by *fluctuating the efficiency* according to the binomial distribution and b) by *changing the grid size* to $\Delta z = 0.066$ (0.133 for π). It is clear that a) reflects the finite MC statistics and we therefore expect and observe deviations of $\Delta p = \pm 0.012$ and $\Delta \xi_{had} = \pm 0.03$, slighly less than half of the statistical error on the data. For b) we find the changes $\Delta p = -0.003$ and $\Delta \xi_{had} = +\ 0.01$ which we attribute to bin fluctuations in the efficiencies and slight differences in sensitivity.

We examine the effect of differing background levels by scaling the separate contributions from ee, $\mu\mu$, $\gamma\gamma$, $q\bar{q}$, $\tau\tau$ and the whole background within the very conservative errors of $\pm 30\%$. We use larger variations than those determined in [10] because we want to show that only grave errors in the background estimates could simulate deviations from $V-A$. The results are summarized in Table 6. The $\mu\mu$ and $q\bar{q}$ contributions have no noticable effect. The largest uncertainty

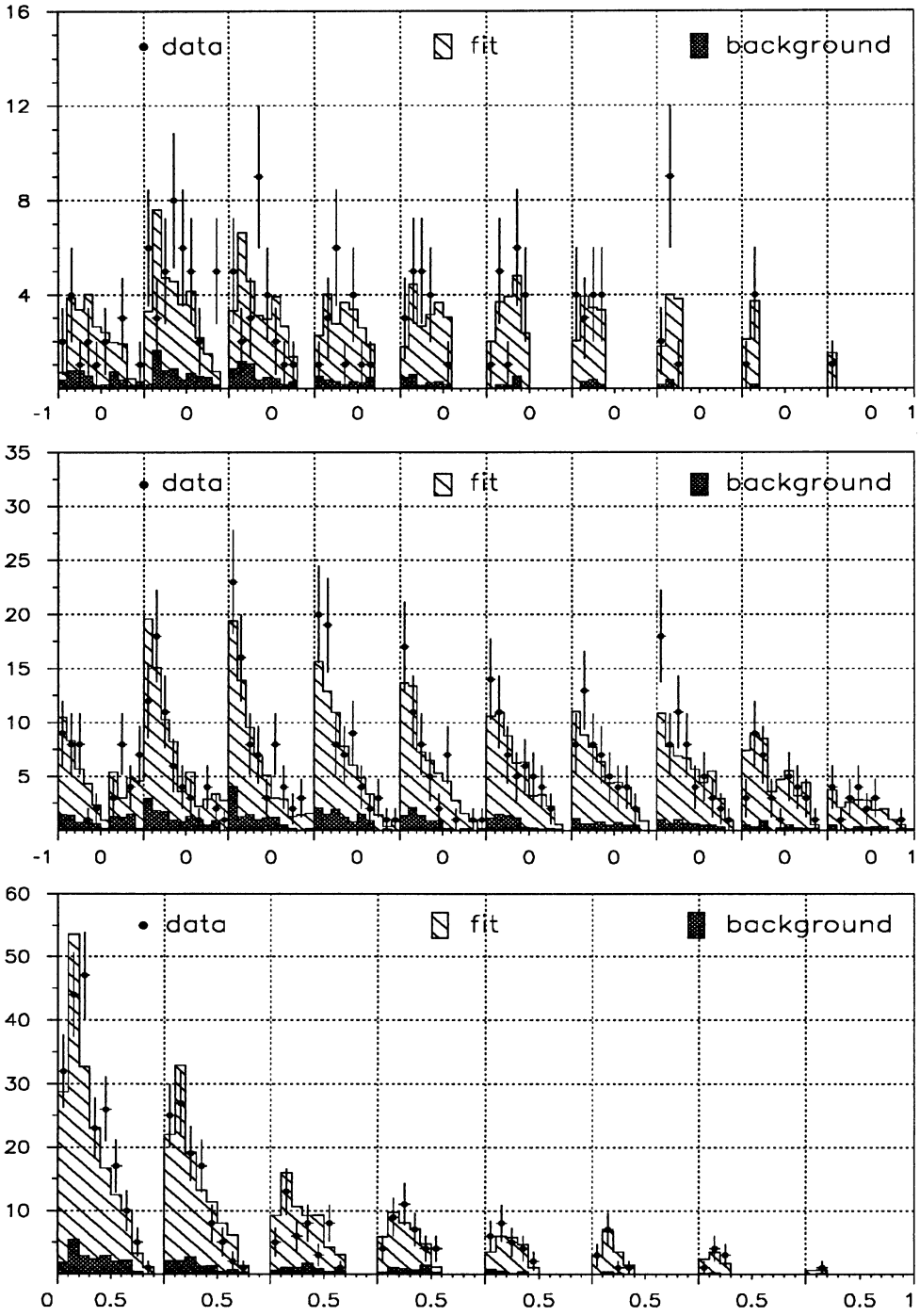

Figure 6: *data, background and fit for $\pi\pi$, $\pi\rho$ and $\rho\rho$ spectra from top to bottom respectively. The symmetric modes are folded across the diagonal (compare with Fig.3).*

is due to variations in the $\tau\tau$ background, $\Delta p = 0.009$ and $\Delta\xi_{had} = 0.01$. On scaling the whole background some shifts cancel each other. Similarly, changes in ξ_π and ξ_ρ tend to be in opposite directions so that ξ_{had} remains almost constant.

MC sample	Δp	$\Delta\xi_\pi$	$\Delta\xi_\rho$	$\Delta\xi_{had}$
ee	0.003	-	-	-
$\gamma\gamma$	0.001	-	-	-
$\tau\tau$	0.009	$^{-0.003}_{+0.01}$	$^{-0.03}_{+0.04}$	$^{-0.01}_{+0.004}$
all	0.009	0.01	0.03	0.01
with LEP constraint				
ee	0.001	0.01	-	-
$\gamma\gamma$	0.001	-	-	-
$\tau\tau$	0.002	$^{-0.02}_{+0.01}$	$^{-0.04}_{+0.02}$	$^{-0.001}_{+0.004}$
all	0.001	0.02	0.02	0.005

Table 6: *Systematic errors from varying the background levels by* $\pm 30\%$. *Some changes cancel out when the whole background is rescaled.*

Differences in resolution and efficiency between MC and data are lumped into an *efficiency slope.* The slopes are almost identical to those in [1], $s_\pi = \pm 0.016$ and $s_\rho = \pm 0.52$, and are tuned to reproduce the changes in polarisation of each mode due to calorimeter modelling problems, TPC and ECAL scale errors, and the π° reconstruction [11]. We apply this correction to each row and column of the ε matrices. Variation of the individual slopes leade to $\Delta p_\pi = \pm 0.016$, $\Delta\xi_\pi \leq \pm 0.01$, $\Delta p_\rho = \pm 0.024$ and $\Delta\xi_\rho = \pm 0.002$. Correcting both particle spectra simultaneously gives in the worst case $\Delta p = \pm 0.021$ and $\Delta\xi_{had} = \pm 0.003$.

By excluding the first bin from the fit we investigate its potential bias. In the π channel this bin has a low efficiency and thus receives a large correction. The observed shifts in the parameters are usually less than the square root of the difference between the square of the errors. Removing the first bin in the ρ channel results in a 1.5σ change of ξ_{rho}. We therefore assign a systematic error

of 0.05 to ξ_{rho}. There are no signficant shifts in ξ_{had}.

Initial state radiation leads to a lower CMS energy and thus to $E_\tau < E_{beam}$. We determine the validity of the assumption by reducing E_τ from E_{beam} in the formulae by 1 and 2 GeV. The consequent changes are negligible, $\Delta p < 0.001$ and $\Delta\xi_{had} < 0.001$.

Table 7 summarizes the systematic errors and their sources. The largest systematic errors are due to the acceptance slope and the finite MC statistics. Adding the various contributions in quadrature yields $\Delta\xi_\pi = 0.055$, $\Delta\xi_\rho = 0.08$ and $\Delta\xi_{had} = 0.035$. Using the LEP constraint the errors on the individual ξ are less: $\Delta\xi_\pi = 0.05$ and $\Delta\xi_\rho = 0.05$.

	Δp	$\Delta\xi_\pi$	$\Delta\xi_\rho$	$\Delta\xi_{had}$
MC statistics	0.012	0.05	0.04	0.03
grid size	0.003	0.02	0.03	0.01
background (±30%)	0.010	0.01	0.03	0.01
slope in ϵ	0.008	0.005	0.02	0.005
fit range	0.010	-	0.05	0.01
initial state rad.	-	-	-	-
sum in quadrature	0.02	0.055	0.08	0.035
with LEP constraint				
MC statistics	0.003	0.045	0.035	0.027
grid size	0.001	0.02	0.03	0.01
background (±30%)	0.002	0.02	0.03	0.005
slope in ϵ	0.002	0.02	0.015	0.02
fit range	-	-	0.01	0.005
sum in quadrature	0.005	0.05	0.05	0.04

Table 7: *Summary of systematic errors.*

8 Summary

We determine the ν_τ–helicity in the decays $\tau \to \pi\nu$, $\rho\nu$ using correlated energy spectra. Our semi-analytical approach is tested on MC and data. On MC it reproduces the input values for the polarisation and the helicity parameter ξ. On data we find a similar polarisation as the standard ALEPH analysis.

Using 18.6 pb^{-1} of data collected in 1990 and 1991 and the additional information from the LEP lineshape measurements, we find $\xi_\pi = -1.00 \pm 0.12 \pm 0.05$ and $\xi_\rho = -1.01 \pm 0.11 \pm 0.05$. Assuming that the neutrinos are identical in both modes we obtain $h(\nu_\tau) = -1.00 \pm 0.07 \pm 0.04$ in agreement with the Standard Model expectation of $h(\nu_\tau) = -1$.

9 The 1992 data

The following shows very preliminary results including the 1992 data. The MC to determine the acceptance and backgrounds are those of 1991.

Comment	p	ξ_π	ξ_ρ	$C(p,\xi_\pi)$	$C(p,\xi_\rho)$	$C(\xi_\pi,\xi_\rho)$	χ^2/NDOF
	-0.131 ± 0.019	-1.01 ± 0.08	-0.94 ± 0.08	-0.16	-0.31	-0.16	1021/ 957
with LEP constraint	-0.139 ±0.011	-1.00 ± 0.08	-0.93 ± 0.08	-0.11	-0.20	-0.18	1021/ 957
		ξ_{had}		$C(p,\xi_{had})$			
	-0.129 ± 0.019	-0.97 ± 0.05		-0.36			1022/ 958
with LEP constraint	-0.139 ±0.011	-0.96 ± 0.05		-0.24			1022/ 958

Table 8: *1990-92 results for the measurement of the ν_τ–helicity with and without the additional information from the 90/91 LEP lineshape measurements. The columns labelled $C(\alpha,\beta)$ give the correlation coefficient.*

References

[1] see also S. Snow, concurrent ALEPH note.

[2] L. Rolandi, *Precision Tests of the Electroweak Interaction*, CERN PPE 92-175, (1992).

[3] L. Michel, Proc. Phys. Soc. London A63, 514 (1950).

[4] K. Mursula and F. Scheck, Nucl. Phys. B253 (1985) 189-204.

[5] ARGUS Collab., Phys. Lett. 250B (1990), 164; Proceedings of the Ohio Workshop 1992.

[6] W.Fetscher, Phys. Rev. D42, (1991) 1544.

[7] C. Nelson, Phys. Rev. D40, (1989), 123; *Erratum:* Phys. Rev. D41, (1990), 2327.

[8] Y. Tsai, Phys. Rev. D4, (1971), 2821.

[9] A. Rougé, Z. Phys. C48, (1990), 75;
K. Hagiwara, et. al., Phys. Lett. B235, (1990), 198.

[10] J. Conway, et al., University of Wisconsin, *Tau and Electron Couplings to the Z from ALEPH*, ALEPH 92-77, PHYSIC 92-68.

[11] ALEPH Collab., *Measurement of Tau Polarisation at the Z Resonanc*, (to be submitted to Z. Phys. C).

[12] S.Jadach and Z. Was, *The Tau Polarization Measurement*, Z Physics at LEP I, CERN 89-08; *Erratum:* 8 March 1990, CERN;
S. Roehn, *Measurement of τ Production and Decay Parameters with the Process $e^+e^- \to Z^0 \to \tau^+\tau^-$; $\tau \to \mu\nu_\tau\nu_\mu$*, Doctoral Thesis, Universität Mainz, (1991).